
MULTI-OBJECTIVE REINFORCEMENT LEARNING FOR CRITICAL SCENARIO GENERATION OF AUTONOMOUS VEHICLES

Jiahui Wu

Simula Research Laboratory and
University of Oslo
Oslo, Norway
jiahui@simula.no

Chengjie Lu

Simula Research Laboratory and
University of Oslo
Oslo, Norway
chengjielu@simula.no

Aitor Arrieta

Mondragon University
Mondragon, Spain
aarrieta@mondragon.edu

Shaukat Ali

Simula Research Laboratory
Oslo, Norway
shaukat@simula.no

ABSTRACT

Autonomous vehicles (AVs) make driving decisions without human intervention. Therefore, ensuring AVs' dependability is critical. Despite significant research and development in AV development, their dependability assurance remains a significant challenge due to the complexity and unpredictability of their operating environments. Scenario-based testing evaluates AVs under various driving scenarios, but the unlimited number of potential scenarios highlights the importance of identifying critical scenarios that can violate safety or functional requirements. Such requirements are inherently interdependent and need to be tested simultaneously. To this end, we propose *MOEQT*, a novel multi-objective reinforcement learning (MORL)-based approach to generate critical scenarios that simultaneously test interdependent safety and functional requirements. *MOEQT* adapts Envelope Q-learning as the MORL algorithm, which dynamically adapts multi-objective weights to balance the relative importance between multiple objectives. *MOEQT* generates critical scenarios to violate multiple requirements through dynamically interacting with the AV environment, ensuring comprehensive AV testing. We evaluate *MOEQT* using an advanced end-to-end AV controller and a high-fidelity simulator and compare *MOEQT* with two baselines: a random strategy and a single-objective RL with a weighted reward function. Our evaluation results show that *MOEQT* achieved an overall better performance in identifying critical scenarios for violating multiple requirements than the baselines.

Keywords Autonomous vehicle testing · Multi-objective reinforcement learning · Driving scenario · Scenario-based testing

1 Introduction

Autonomous vehicles (AVs) automatically navigate and make driving decisions without human intervention, aiming to achieve safe, efficient, and fully automated transportation. At the same time, it remains challenging to ensure AVs' dependability before their deployment in the real world due to the complexity of AVs and their driving environments. Scenario-based AV testing [1, 2, 3, 4, 5, 6, 7] offers a practical way to evaluate AVs under various driving scenarios, which is a critical step toward the successful deployment of AVs. However, given the complexity of AVs and the uncertainty of their driving environments, the number of possible driving scenarios for testing AVs is theoretically infinite. Therefore, it is paramount to find critical scenarios that lead the AV to misbehave by violating safety or functional requirements.

Scenario-based testing methods generate critical scenarios within driving environments simulated by high-fidelity simulators such as CARLA [8]. A test scenario is defined by a set of environmental parameters that characterize

static and dynamic objects (e.g., vehicles, pedestrians, and other obstacles) in the AV’s environment. These scenarios are specifically designed to reveal potential safety or functional requirements violations. Existing methods generate critical scenarios by exploring complex search spaces covering various driving scenarios. To this end, search-based techniques [9, 10, 11, 12] have been predominant for AV testing, designed to handle large search spaces and identify critical scenarios guided by fitness functions. However, such approaches show limited effectiveness in dealing with runtime sequential interactions, which are essential when manipulating dynamic objects and ensuring precise control over them. Besides, the environment in which an AV operates is constantly changing and uncertain, while search-based approaches typically do not interact with or learn from the environment during the search process. Instead, they consider the environment as independent when searching for scenarios and then execute scenarios in the environment, and therefore cannot effectively adapt to environmental changes.

Recently, reinforcement learning (RL) [13] has been proven to be a promising technique for scenario-based AV testing. Inheriting the features of RL agents in adaptive control and dynamic interaction, RL-based testing approaches [14, 15, 16] generate critical scenarios by interacting with the environment at runtime and can be adaptive to dynamic environmental changes. However, RL-based methods typically focus on detecting safety violations, such as collisions, whereas the functional requirements are less tested. Thus, it is crucial to adaptively generate critical scenarios to simultaneously test safety and functional requirements. A relevant work is MORLOT [15], which adapts single-objective RL and many-objective search to generate test suites to violate as many requirements as possible. MORLOT is designed to violate multiple *independent* requirements by generating a set of scenarios, each focusing on violating one independent requirement. However, in practice, many requirements are interdependent and must be evaluated simultaneously to ensure comprehensive testing. For instance, safety requirements such as avoiding collisions could be closely related to functional requirements like maintaining lane positioning or completing routes within a time budget. Violating functional requirements (e.g., failing to complete routes) may compromise safety requirements (e.g., causing a collision), highlighting the need for approaches simultaneously evaluating multiple requirements. To this end, in this work, we aim to test multiple interdependent requirements for which multi-objective RL (MORL) [17] is suitable.

MORL learns control policies to optimize multiple criteria simultaneously. Compared to single-objective RL, MORL handles trade-offs among multiple objectives, e.g., safety and performance, to solve time-series decision-making problems in complex environments [17, 18]. MORL has shown effectiveness in various domains, such as robotics [19] and autonomous driving [20]. Motivated by the challenges of handling interdependent requirements in RL-based AV testing and the success of MORL, we propose *MOEQT*, a novel MORL-based AV testing approach. *MOEQT* generates critical scenarios to test multiple requirements by interactively and adaptively configuring the AV operating environment. Specifically, *MOEQT* employs Envelope Q-learning (EQL) [21], a generalized MORL algorithm that learns a single policy network to optimize multiple objectives by dynamically adjusting the agent’s preferences (i.e., the relative importance assigned to each objective) during the training phase. *MOEQT* learns by observing the environment status and then taking actions to manipulate objects in the environment at each time step. *MOEQT* formulates the violation of each requirement as an objective function. The values from these objective functions are then used by the reward function to guide the MORL agent towards generating scenarios that can violate multiple requirements. We evaluate *MOEQT* using an end-to-end AV controller (i.e., Interfuser [22]) and a high-fidelity simulator (i.e., CARLA [8]). We compare *MOEQT* with two baselines: a random strategy and a single-objective RL with a weighted reward function, and select six roads covering various driving conditions for the experiment. The evaluation results show that *MOEQT* is more effective in generating critical scenarios that violate multiple requirements simultaneously.

To summarize, the contributions of this paper are: 1) To test multiple interdependent AV requirements, we propose a novel MORL-based approach, *MOEQT*, that generates critical scenarios to violate multiple requirements by adaptively configuring the AV’s operating environment; 2) We formulate the AV testing problem using a multi-objective Markov decision process (MOMDP) and solve it using the EQL algorithm; 3) We conduct an empirical evaluation and compare *MOEQT* with two baselines. The results show that *MOEQT* outperforms baselines in terms of violating multiple requirements simultaneously and achieves a more balanced performance in optimizing multiple objectives.

2 Background

2.1 Reinforcement Learning

Reinforcement learning (RL) learns an optimal policy for an agent to perform tasks through interacting with the environment to maximize cumulative rewards [13]. Unlike supervised learning, which uses labeled data to train models, RL requires no prior knowledge and learns through trial and error. Specifically, in RL, an agent observes the current state of the environment, selects actions based on the policy, and receives a reward signal as feedback for its decision. A typical RL process can be formulated as a Markov decision process (MDP), which is a 4-tuple $\langle \mathcal{S}, \mathcal{A}, \mathcal{P}, \mathcal{R} \rangle$ with state space \mathcal{S} specifying the possible situations of the environment, action space \mathcal{A} defining possible actions the

agent can take, transition distribution $\mathcal{P}(s_{t+1}|s_t, a_t)$ specifying how the environment state changes in response to the agent’s action, and reward function $\mathcal{R}(s_t, a_t)$ measuring the agent’s performance of taking an action. In MDP, the agent interacts with the environment at each discrete time step. Specifically, at each time step t , the agent observes the current state of the environment as $s_t \in \mathcal{S}$ and then selects an action $a_t \in \mathcal{A}$ to perform based on s_t and the behavioral policy. After the action is finished, the agent receives a reward $r_t \sim \mathcal{R}(s_t, a_t)$ as feedback to evaluate the agent’s performance, and the environment moves into a new state $s_{t+1} = \mathcal{P}(s_{t+1}|s_t, a_t)$. RL aims to find an optimal policy $\pi^*(a_t|s_t)$, a mapping from state to probabilities of selecting actions, to maximize the expected cumulative reward over time. Q-learning [23] is a classical RL algorithm that learns via an action-value function called Q-value function:

$$Q^\pi(s_t, a_t) = \mathbb{E}_\pi[R_t|s_t, a_t]. \quad (1)$$

The Q-value of the state-action pair (s_t, a_t) estimates the expected future reward by taking action a_t in state s_t with policy π . Q-value is updated based on the Bellman function:

$$Q^\pi(s_t, a_t) = \mathbb{E}_\pi[r_t + \gamma \max_{a_{t+1}} Q^\pi(s_{t+1}, a_{t+1})], \quad (2)$$

where γ is the discount factor determining how much future rewards contribute to immediate rewards.

Traditional RL algorithms, such as Q-learning, are designed to address tasks with a single long-term objective. However, many real-world tasks involve multiple criteria that must be optimized simultaneously. For example, when designing AVs, ensuring safety and passenger comfort is paramount. To this end, MORL, which learns optimal policies to handle two or more objectives, has become an important research area.

2.2 Multi-Objective Reinforcement Learning

MORL aims to solve sequential decision-making problems where multiple objectives must be considered [24]. A MORL process can be formulated as an MOMDP, an extension of MDP. Unlike MDP calculating a single scalar reward r , the reward function in MOMDP returns a vector \mathbf{r} containing the rewards for each objective. The action-value function in MORL is a vectored Q-function:

$$\mathbf{Q}^\pi(s_t, a_t) = [Q_1^\pi(s_t, a_t), Q_2^\pi(s_t, a_t), \dots, Q_{NO}^\pi(s_t, a_t)]^T, \quad (3)$$

where NO is the number of objectives and for the i_{th} objective, its corresponding action-value function is $Q_i^\pi(s_t, a_t)$, which is updated using the Bellman function 2. MORL can be classified into two types based on how they find the optimal policy. The first class is single-policy MORL, aiming to find one optimal policy that represents the weights among the multiple objectives. The second class is multi-policy or Pareto-based MORL, which finds a set of policies that approximate the Pareto front. Each policy balances different objectives and no single policy can dominate another across all objectives.

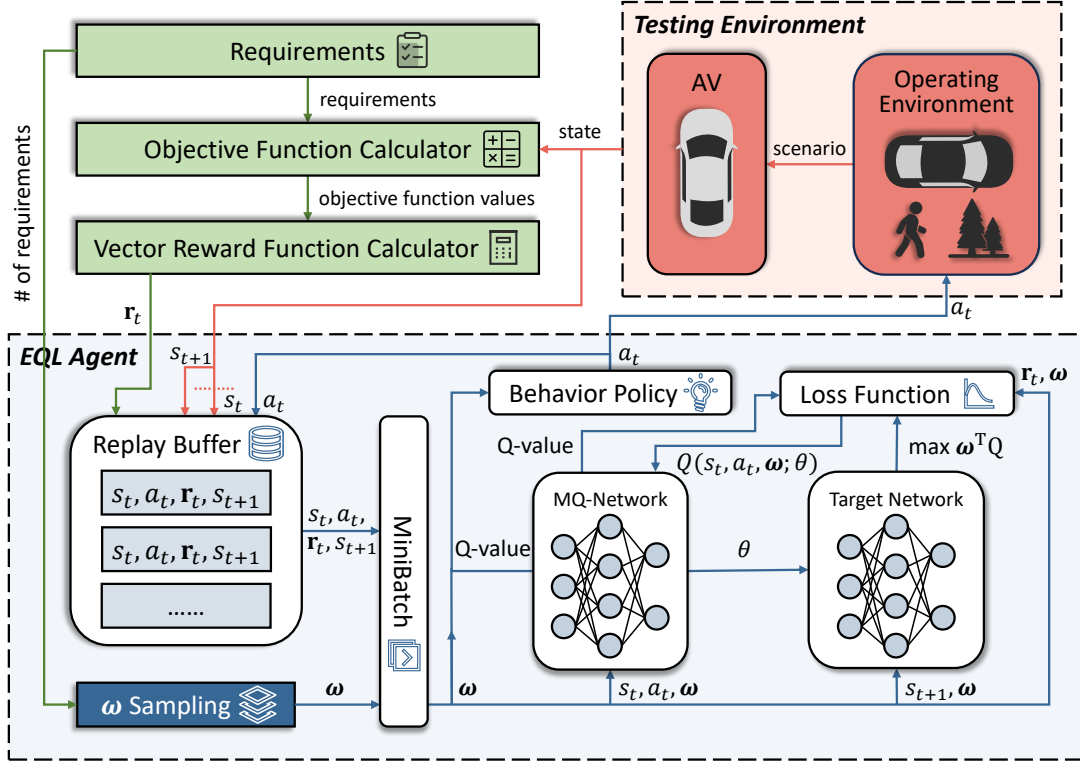
In this paper, we employ a single-policy MORL called EQL [21] given its success in multi-objective RL tasks such as Games and Robot control [25]. In EQL, an MOMDP is represented using a 6-tuple $\langle \mathcal{S}, \mathcal{A}, \mathcal{P}, \mathbf{R}, \Omega, f_\Omega \rangle$, where \mathcal{S} , \mathcal{A} , and \mathcal{P} are the same as in traditional MDP. Notably, $\mathbf{R}(s_t, a_t)$ represents a vector reward function, Ω is the space of weights of multi-objectives, and f_Ω is linear weight functions, each of which produces a scalar utility using the weight $\omega \in \Omega$. The goal of EQL is to learn a single policy network that can be generalized across the entire weight space. One EQL implementation is based on Deep Q-learning (DQN) [26], a classical single-objective RL that uses a deep neural network called Q-network to approximate and store Q-values. EQL extends Q-network into a multiple-objective Q-network (MQ-network). Unlike Q-network, which takes only the state as input, MQ-network takes the concatenation of the state and the weight as input. Additionally, EQL employs homotopy optimization [27] to adaptively adjust the loss function computation using weight vectors. These designs allow EQL to dynamically learn weights to optimize objectives that may vary in importance. By leveraging adaptive weights during training, EQL effectively balances the relative importance between different objectives, enhancing its ability to generalize across diverse problems.

3 Approach

3.1 MOEQT Overview

Figure 1 shows an overview of how *MOEQT* generates critical scenarios to test multiple requirements simultaneously. Given a set of requirements, *MOEQT* employs EQL as the MORL solution to learn operating environment configurations to violate these requirements. Such environment configuration characterizes a critical scenario, i.e., a test scenario in which the AV simultaneously violates multiple requirements.

MOEQT builds a testing environment consisting of the AV and its operating environment. As Figure 1 shows, to configure the operating environment of the AV, at each time step t , the EQL agent observes the current state s_t from


 Figure 1: Overview of AV Testing with *MOEQT*

the testing environment, which contains the state of both the AV and its operating environment. The agent then samples a vector of multi-objective weights ω_t based on the number of requirements targeted for violation. Taking the concatenation of s_t and ω_t as input, the MQ-network computes the corresponding Q-values. Based on these Q-values and the weight vector ω_t , the behavior policy decides an action a_t to configure the AV's operating environment. The AV navigates in the newly configured environment for a specified period, during which the objective function calculator computes values in real-time based on the objective functions designed for each requirement violation, considering the state of the AV and the environment. These values are then fed into the vector reward function calculator for vector reward computation. After the AV reaches time step $t + 1$, i.e., a_t is finished, the EQL agent observes the next state s_{t+1} . The vector reward function calculator then calculates the corresponding vector reward \mathbf{r}_t for the triplet (s_t, a_t, ω_t) based on the objective function values during time step t . The agent then constructs a transition tuple $\langle s_t, a_t, \mathbf{r}_t, s_{t+1} \rangle$ and stores it in a replay buffer using a specific replay mechanism. Notice that ω_t is decoupled from the transition, which allows for sample-efficient learning by using the prioritized experience replay scheme [28]. Once the replay memory is full, a minibatch sampled from the replay buffer, along with randomly sampled weights, are used to update the MQ-network. To ensure stability when training the MQ-network, a separate target network with identical architecture as the MQ-network is used to generate target Q-values for loss calculation. Its parameters are clones from the MQ-network every fixed number of steps. Finally, *MOEQT* terminates an episode when the AV either completes its route, collides with other objects, or reaches the time limit (timeout).

3.2 Problem Definition

AVs have to meet a variety of safety and functional requirements that are not only for AVs but also for the environments in which they operate. Consequently, complex interdependencies exist among the requirements, making it ineffective to consider each requirement in isolation, e.g., for testing. Thus, to ensure the AV's safety and functionality, it is essential to validate safety and functional requirements simultaneously. To achieve this, scenario-based testing is employed to generate critical scenarios to violate various requirements, providing AV developers with a comprehensive testing solution.

Particularly, assume that given an AV, $Req = \{req_1, req_2, \dots, req_n\}$ is a set of its safety and functional requirements, and each $req_i \in R$ represents a specific requirement that the AV must satisfy. For example, the AV should not collide

with any object. Our goal in AV testing is to generate a critical scenario sc using a function g to simultaneously violate the requirements in Req . Formally, this can be expressed as $sc = g(AV, Req)$, where AV is the AV under test and Req is the set of requirements that need to be met. To construct sc , along with the AV under test, the environment must be modeled. Let $E = \{E_{static}, E_{dynamic}\}$ be the environment, where E_{static} represents a set of static objects within the scenario that remains static over time, e.g., trees and traffic signs, and $E_{dynamic}$ denotes dynamic objects in the scenario that may change over time, such as non-player character (NPC) vehicles and pedestrians. Static objects, defined as O' , in E_{static} are the objects that remain unchanged over time. Let N be the number of static objects in the environment, where E_{static} can be expressed as $E_{static} = \{O'_1, O'_2, \dots, O'_N\}$. Their configurations, denoted as $C^{O'}$, can be represented using their states such as positions and rotations. In contrast, dynamic objects, defined as O , in $E_{dynamic}$ change over time, so their configurations C^O must account for both their states and behaviors over time. Let M be the number of dynamic objects in the environment, where $E_{dynamic}$ can be represented as $E_{dynamic} = \{O_1, O_2, \dots, O_M\}$.

To represent the dynamic changes in the environment over time, the states and behaviors of dynamic objects in $E_{dynamic}$ can be tracked across a sequence of time steps. Let T be the total number of time steps and t be the current time step, where $t \in \{1, 2, \dots, T\}$. Then $E_{dynamic}$ can be expressed as a time-sequenced set, described as $E_{dynamic} = \{E_{dynamic}(t) | t \in \{1, 2, \dots, T\}\}$. Specifically, $E_{dynamic}(t)$ represents a set of dynamic objects at the time step t , which is defined as $E_{dynamic}(t) = \{O_1, O_2, \dots, O_{M_t}\}$, where M_t denotes the number of dynamic objects in the environment at the current time step t . O_{M_t} contains the set of configurations for the dynamic object that changes over instants within the time step t . Assuming each time step contains m instants, we define t_j as the j th instant within the time step t , and O_{M_t} can be described as $O_{M_t} = \{C_{t_j}^{O_{M_t}} | j \in \{1, 2, \dots, m\}\}$, where $C_{t_j}^{O_{M_t}}$ is the configuration of the dynamic object O_{M_t} at instant j within the time step t . Note that the dynamic environment of each time step ($E_{dynamic}(t)$) is influenced by the previous time step ($E_{dynamic}(t-1)$), with the configurations of all dynamic objects at the final moment of the prior time step (i.e., at the instant m within the time step $t-1$) continuously affecting the dynamic environment of the next time step.

3.3 Requirements and Objective Functions

To quantify the degree or probability of violation for each requirement req_i in the set $Req = \{req_1, req_2, \dots, req_n\}$ associated with an AV, we define a set of objective functions $H = \{h_1, h_2, \dots, h_n\}$. Each function h_i measures the degree or probability of violation associated with the corresponding $req_i \in Req$ and can be expressed as $h_i(req_i) = \text{Measure of violation for requirement } req_i, i \in \{1, 2, \dots, n\}$. For instance, assuming one of the requirements for the AV is "the AV should complete the route within a time budget", its corresponding objective function measures the percentage of the route completion. A smaller value of this objective function (i.e., a smaller route completion percentage) indicates a higher degree of violation. Thus, given a set of requirements Req , a critical scenario $sc = g(AV, Req)$ is defined as the scenario that satisfies: $\forall req_i \in Req : sc \text{ violates } req_i$.

3.4 Formulating AV Testing as an MOMDP

We model the MORL-based AV testing problem as an MOMDP as mentioned in Section 2.2, which is defined as a 6-tuple $\langle \mathcal{S}, \mathcal{A}, \mathcal{P}, \mathbf{R}, \Omega, f_\Omega \rangle$. Specifically, \mathcal{P} indicates the transition distribution, Ω describes the space of weights, and f_Ω expresses the weight functions. For AV testing, we adopt the default definitions for these components, while reformulating the state space \mathcal{S} , action space \mathcal{A} , and vector reward function \mathbf{R} as follows:

3.4.1 State Space

In MORL, the state space represents all the possible configurations of the environment that can be perceived and understood by the agent. Effective state encoding captures the critical information from the environment, enabling the agent to make appropriate decisions. For AV testing, a commonly used state encoding focuses on the AV and its operating environment [29]. Thus, the state space can be formulated based on the configuration of the AV and its environment and can be represented as $\mathcal{S} = \{C^{AV}, \{C^{O'_i}\}_{i=1}^N, \{C^{O_j}\}_{j=1}^M\}$, where N is the number of static objects, and M is the number of dynamic objects. Notably, C^{AV} means the configuration of the AV, $C^{O'_i}$ is the configuration of the i th static object, and C^{O_j} is the configuration of the j th dynamic object. Based on the formulated state space, the MORL agent can observe the specific state at each time step t , which is denoted as $\{C_t^{AV}, \{C_t^{O'_i}\}_{i=1}^N, \{C_t^{O_j}\}_{j=1}^M\}$.

3.4.2 Action Space

\mathcal{A} encompasses all possible actions available to the MORL agent, defining the range of decisions it can make in a given state and directly determining the impact on the environment. At each time step t , the agent observes the current state $\{C_t^{AV}, \{C_t^{O_i}\}_{i=1}^N, \{C_t^{O_j}\}_{j=1}^M\}$ and select an appropriate action from the action space to transition the system to the next state $\{C_{t+1}^{AV}, \{C_{t+1}^{O_i}\}_{i=1}^N, \{C_{t+1}^{O_j}\}_{j=1}^M\}$. This action involves manipulating objects in the AV testing environment, such as introducing dynamic objects or adjusting their configurations, thereby altering the environment to interact with the AV. These changes can create conditions that increase the likelihood of the AV making driving decisions that violate specified requirements.

3.4.3 Vector Reward Function

In MORL, \mathbf{R} typically represents a vector reward function, with each reward function computing the reward value for a specific objective separately. After executing an action in the current state, the MORL agent receives a vector \mathbf{r} containing rewards corresponding to multiple objectives, which guides the agent in updating the weights for multiple objectives and balancing their relative importance. For AV testing, \mathbf{R} is formulated based on the objective functions defined in Section 3.3. The objective functions $H = \{h_1, h_2, \dots, h_m\}$ assess the degree or probability of violations of requirements for each instant within every time step. On the other hand, the vector reward function focuses on each time step and is derived by identifying the maximum value of each objective function within that time step, ultimately forming the vector reward function required for MORL. Let t be the current time step and $\mathbf{R}(t)$ be the vector reward function at time step t . Then, $\mathbf{R}(t)$ can be expressed as $\mathbf{R}(t) = [\max(h_{i-t_j} | j \in \{1, 2, \dots, m\}) \text{ for } i \in \{1, 2, \dots, n\}]$, where h_{i-t_j} represents the i th objective function at instant j within time step t . Specifically, if each time step contains only one instant, the vector reward function will be equivalent to the objective functions.

4 Experiment Design

4.1 Research Questions

In our evaluation, we will answer the following two Research Questions (RQs):

- **RQ1:** *How does MOEQT perform compared to a random approach?* We aim to assess whether the targeted problem is complex and cannot be solved by a simple, random approach.
- **RQ2:** *How does MOEQT perform compared to single-objective RL with a weighted reward function?* Single-objective RLs are simpler algorithms than the one we used. The goal of this RQ is to see whether there is justification for selecting a multi-objective RL instead of relying on a single-objective RL algorithm that casts the problem as a single-objective approach (i.e., by using a weighted reward function).

4.2 Subject System and Simulator

We employ Interfuser [22] as the subject system, which is an advanced end-to-end AV controller on the CARLA leaderboard. Interfuser is a safety-enhanced framework based on the Transformer architecture [30] for comprehensive scene understanding and safe autonomous driving. It employs a multimodal sensor fusion transformer encoder to integrate sensor data from multiple RGB cameras and a LiDAR sensor. Then, it uses a transformer decoder to generate driving actions and interpretable intermediate features. Finally, a safety controller processes the interpretable intermediate features to refine and enhance the safety of the driving actions. Interfuser has been evaluated in extensive driving scenarios, from urban environments to highways, demonstrating its outstanding safe driving performance. Regarding the simulator, we adopt CARLA [8], a high-fidelity open-source autonomous driving simulator. CARLA provides an extensive list of digital assets, such as vehicles, sensors and high-definition maps to support AV development, training, and validation. In the evaluation of *MOEQT*, we use CARLA-0.9.10.1 and its default Interfuser settings. We choose the default vehicle used by Interfuser, which is a Tesla Model 3.

4.3 Baselines

We employ two comparison baselines to evaluate *MOEQT*: a random strategy (*RS*) and a single-objective RL with a weighted reward function (*SORLW*). Specifically, *RS* randomly selects an action from the action space to configure the environmental objects at each time step. *SORLW* learns the optimal policy following a classical MDP process. At each time step, it first observes a state from the environment and then selects an action to perform based on the state and the behavioral policy. After the execution of the action, a reward is returned and the environment enters a new

state. *SORLW* follows the same design of state space and action space as *MOEQT*. However, unlike *MOEQT*, which adapts multiple reward functions, *SORLW* weights all reward functions into one reward function using equal weight. The implementation of *SORLW* is based on Deep Q-learning [26], a classical RL algorithm that has demonstrated good performance in solving complicated sequential decision-making problems, such as robotics kinematics [31], AV control [32], and AV testing [14].

4.4 Experiment Setup

4.4.1 Instantiation of Requirements and Objective Functions

While our approach is generic to any AV requirement, in our evaluation, we consider two interdependent requirements, one of which is safety-critical, whereas the second is a functional requirement. We then develop corresponding objective functions for AV testing based on these requirements. The following are the safety and functional requirements we cover:

- *R1*: The AV should not collide with any object.
- *R2*: The AV should complete its route within a time budget.

R1 emphasizes that the AV must avoid collisions with any object in the environment, including static and dynamic obstacles. This requirement ensures AV safety and prevents traffic accidents [33]. To quantify the violation of this requirement, we use *Time to Collision (TTC)* [34] as an objective function. *TTC* represents the remaining time before the AV collides with another object, assuming both maintain their current collision route and velocity difference, which is defined as:

$$TTC = \frac{d_{rel}}{v_{rel}}, \quad (4)$$

where d_{rel} means the relative distance between the AV and another object in the environment, and v_{rel} calculates the relative velocity of the AV to another object. The value of *TTC* ranges from 0 to positive infinity. A lower *TTC* indicates a higher possibility of violating *R1*. Specifically, when *TTC* is 0, it means the AV has collided with another object, completely violating *R1*. We can perform real-time calculations on *TTC*, offering insights into the likelihood of potential collisions and enhancing the testing of AV driving safety. Note that, for simplicity, we provide a general formulation for *TTC*; however, in our implementation, we compute the actual *TTC* based on the specific position and velocity vectors of the AV and objects within the scenario.

The *R2* requirement demonstrates our focus on the functional aspects of the AV. It requires the AV to complete the planned route within a specified time budget, which involves real-time environmental awareness and path planning to dynamically adapt to complex scenario changes, verifying the AV’s driving reliability [35]. To assess this requirement, we employ *Route Completion (RC)* [36] as an objective function, measuring the percentage of route successfully completed by the AV. *RC* is defined as follows:

$$RC = \frac{d_{driven}}{D_{total}} \times 100\%, \quad (5)$$

where d_{driven} measures the actual distance traveled by the AV along a given route, and D_{total} denotes the total length of the entire test route. The value of *RC* ranges from 0% to 100%, with 100% indicating that the AV has successfully completed the specified route. By measuring *RC*, we can assess the AV’s execution efficiency and the stability and reliability of its global or local path planning in dynamic driving conditions. Thus, for AV testing, we expect a lower *RC*, which indicates a higher likelihood of the violation of *R2*. Note that if *RC* stays at 0% continuously, it indicates that the AV is either unresponsive or remains stopped, which should be avoided in the implementation as it may result in an ineffective test.

4.4.2 Configurable Environment Parameters

When applying scenario-based testing to AVs, some degree of abstraction is needed, as considering all environmental factors that occur in reality would require enormous computing power, making our approach non-scalable. We therefore prioritize, for our study, the configuration and analysis of dynamic objects, i.e., NPC vehicles and pedestrians, although it could easily be extended to factors that could be of interest to AV developers.

The configurable parameters of an NPC vehicle can be represented by a triplet: $(dis_v^{la}, dis_v^{lo}, bhv_v)$, where dis_v^{la} and dis_v^{lo} means the lateral and longitudinal distances between the NPC vehicle and the AV, respectively. Meanwhile, bhv_v indicates the driving behavior of the NPC vehicle. In our implementation, to simplify the problem and enhance the experimental efficiency, based on the results of our pilot study and supported by findings in related research [37], we

sample the value of dis_v^{la} from the discrete list $[-20, 0, 20]$ and dis_v^{lo} from $[-3.5, 0, 3.5]$. The behavior bhv_v can be one of three options: changing lanes to the left, changing lanes to the right, or maintaining the current lane. For example, if $(dis_v^{la}, dis_v^{lo}, bhv_v)$ is set to $(-20, 3.5, \text{changing lanes to the left})$, it means that a new NPC vehicle will be generated 20 meters directly behind the AV and 3.5 meters to the right, with its behavior set to prepare for a left lane change. Note that the travel direction of the newly generated NPC vehicle is set to align with the designated direction of the road it is on. Particularly, the lateral distance of 20 meters ensures the generated NPC vehicle maintains a safe proximity to the AV without being too far, which could invalidate the test. Similarly, the longitudinal distance of 3.5 meters matches the road width in the CARLA simulator, ensuring the NPC vehicle is neither too close nor too far from the AV. We exclude the configuration where (dis_v^{la}, dis_v^{lo}) is $(0, 0)$, resulting in a total of 24 distinct configurations for the NPC vehicles.

On the other hand, the feature of a pedestrian can be described as a quadruplet: $(dis_p^{la}, dis_p^{lo}, dir_p, spd_p)$. Similarly to the NPC vehicle, dis_p^{la} and dis_p^{lo} reflect the lateral and longitudinal distances between the pedestrian and the AV. dir_p controls the forward direction of the pedestrian. Lastly, spd_p sets the constant speed of the pedestrian. More specifically, the lateral distance dis_p^{la} is fixed at 10 meters ahead of the AV’s direction of travel, while the longitudinal distance dis_p^{lo} is selected from a discrete list $[-10, 10]$. Similarly, to ensure the newly generated pedestrians maintain a safe distance from the AV, we fix the distance at 10 meters. The pedestrian’s direction dir_p can be 45 degrees aligned, 45 degrees opposite, or 90 degrees perpendicular to the AV’s travel direction, while ensuring the pedestrian faces the AV. As for the pedestrian’s speed, i.e., spd_p , it is set to either 0.94 meters per second (average walking speed) or 1.43 meters per second (average running speed). In total, we can set a pedestrian with 12 different configurations.

Additionally, to ensure the realism of the generated objects in the scenario, we apply specific realistic constraints. As previously mentioned, NPC vehicles and pedestrians are placed at a safe distance from the AV. Besides, newly generated objects are also positioned at a safe distance from other NPC vehicles or pedestrians already present in the scenario. All objects are confined within the boundaries of the map on which the AV is traveling and are generated on appropriate roads (e.g., lanes) specified by the simulator, preventing unrealistic placements (e.g., on top of a tree). Moreover, the driving direction of newly generated NPC vehicles is aligned with the designated road direction, and once initialized, these NPC vehicles are controlled by the simulator’s default autopilot algorithm. It ensures realistic vehicle generation and driving behavior. For pedestrians, which are configured to always face the AV, we prevent invalid test scenarios where they might intentionally collide with the AV or other vehicles. Based on pilot study results, a perceived safe walking distance is set. If pedestrians come within this distance of other objects, they will stop immediately to prevent any intentional collisions. In addition, the speeds of NPC vehicles and pedestrians are strictly regulated. NPC vehicles are capped at the maximum speed limit corresponding to the road they are on, which can be obtained from the simulator, while pedestrian speeds are set to either the average walking or running speed.

4.4.3 MOMDP Instantiation

State Space. We dynamically configure environment parameters in the simulator to generate new dynamic objects, leading to a constantly evolving set of object configurations over time. Leveraging the parameters available from the CARLA simulator, we define the specific state at each time step as a quintuple $\langle pos, rot, vel, acc, anv \rangle$. Specifically, each element of the state represents the AV’s current position, rotation, velocity, acceleration, and angular velocity, respectively, with each element being a vector of three components. For instance, position pos can be defined as $pos = (x, y, z)$, and rotation rot is expressed as $rot = (\theta, \psi, \phi)$. Thus, each observed state will contain 15 state parameters.

Action Space. We define each action as the configuration of a new dynamic object in the environment to increase the complexity of the scenario for AV testing. As mentioned in Section 4.4.2, dynamic objects fall into two categories: NPC vehicles and pedestrians. We have 24 different configurations for NPC vehicles and 12 discrete configurations for pedestrians, resulting in an action space size of $24 + 12 = 36$. Thus, the action space consists of 36 possible actions, each used to create a configured dynamic object for AV testing.

Vector Reward Function. As mentioned in Section 4.4.1, we focus on two key safety and functional requirements. Correspondingly, we define the objective functions TTC and RC , where lower values indicate a higher degree or possibility of requirement violations. However, in $MOEQT$, higher rewards motivate the EQL agent to continue behaviors that generate those rewards to optimize objectives. Therefore, to increase the likelihood of the AV violating the requirements for testing, we define the corresponding reward functions as follows:

$$Reward_{TTC} = \begin{cases} 1, & \text{if collision occurs,} \\ nor\left(\frac{1}{1 + \log(TTC + 1)}\right), & \text{otherwise.} \end{cases} \quad (6)$$

$$Reward_{RC} = \begin{cases} 1 - nor(RC), & \text{if } RC \neq 0, \\ 0, & \text{otherwise.} \end{cases} \quad (7)$$

We consider all requirements equally important, so we use a normalization function $nor()$ to scale both $Reward_{TTC}$ and $Reward_{RC}$ within the range $[0, 1]$, ensuring fairness. Based on our pilot study, we observed that most TTC values fall between 0 and 20, with some exceeding 20. To better capture variations in smaller TTC values, we apply a logarithmic function to scale the data, enhancing its utility. Besides, if a collision occurs, we set $Reward_{TTC}$, which measures AV safety, to the maximum value of 1, emphasizing the significance of collisions in the test. Additionally, to prevent the generated scenario from causing the AV to remain stationary, leading to an invalid test, we set $Reward_{RC}$ to 0 when RC remains consistently 0. Accordingly, the vector reward function of *MOEQT* is defined as $\mathbf{R} = [Reward_{TTC}, Reward_{RC}]$, guiding the EQL agent in selecting appropriate actions to generate critical scenarios.

4.4.4 Network Architecture, Parameter Settings and Implementation

To ensure the effectiveness of *MOEQT* and baseline methods for a fair comparison, a suitable network architecture and corresponding parameter settings need to be selected. For this purpose, we employed an automated hyperparameter optimization framework, Optuna [38], and conducted pilot studies to optimize both the network architecture and parameter settings. The detailed implementation can be found in our publicly available repository [39].

Based on the original EQL implementation [21] and a tool called MORL-Baselines [25], we implemented *MOEQT*. We adopt the ϵ -greedy policy [40] to balance exploration and exploitation of the action space and utilize the prioritized experience replay [28] to store transition tuples. Additionally, we apply homotopy optimization [27] for calculating the loss function. Meanwhile, *SORLW* employs the same implementation as DeepCollision, proposed by Lu et al. [14], which has demonstrated effectiveness in testing AVs using RL.

For model training, based on Optuna’s tuning results and our pilot study, we executed 1200 episodes, each consisting of 6 time steps, with 40 CARLA simulator minimum unit times allocated for each time step. To account for the stochastic nature of our method and selected baselines, during the model evaluation phase, we executed 100 episodes for both *MOEQT* and *SORLW*, freezing the training-related parameters while keeping the remaining parameters unchanged.

4.4.5 Roads

MOEQT generates critical scenarios by configuring the driving environment of the AV throughout the driving task. In this work, we specify the driving tasks using different roads with various road structures. Each road has a starting and end point specifying the route of the AV. Specifically, as Figure 2 shows, we select six roads for the experiment, covering the six scenario categories on the CARLA Leaderboard [36]. These categories are instances of the pre-crash scenarios from NHTSA pre-crash typology [41].

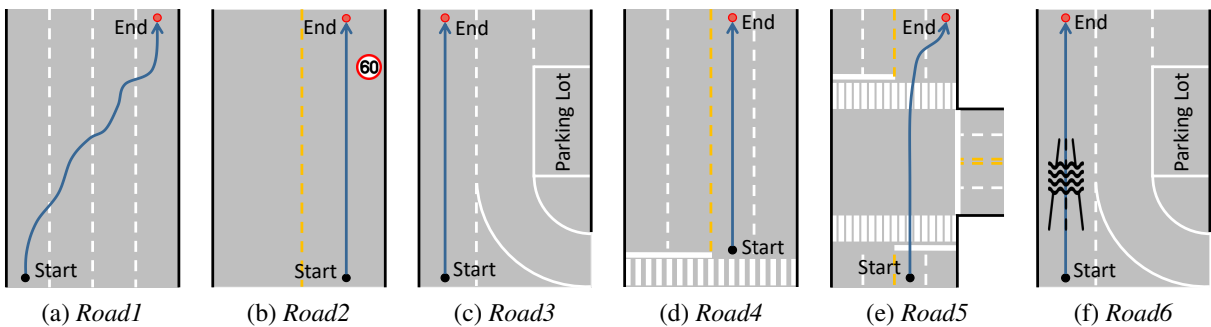


Figure 2: Driving roads for specifying driving tasks.

4.5 Evaluation Metrics

To answer RQs, we defined the following metrics, which allowed us to compare *MOEQT* with the selected baselines:

V_{R1} assesses the number of *R1* requirement violations, which occurs when the AV collides with other objects. This metric is measured by the number of generated scenarios resulting in collisions.

V_{R2} evaluates the number of $R2$ requirement violations, triggered when the AV either fails to complete the specified route within a given time budget or is involved in a collision. It is calculated based on the number of scenarios where this requirement is entirely violated.

V_{R1_R2} quantifies the number of generated scenarios that violate both requirements simultaneously, providing a direct assessment of the method’s effectiveness in violating $R1$ and $R2$ simultaneously.

Note that all V metrics are expressed on a scale of 0 to 100. A value of 0 indicates no critical scenarios violating the corresponding requirement(s), and a value of 100 means that all generated scenarios violate the associated requirement(s).

TTC measures the time remaining until the AV collides with other objects, assuming their current velocity and collision course stay constant. This metric quantifies the degree of violation of requirement $R1$, using the same computation as in Equation 4. It ranges from 0 to positive infinity, with a value closer to 0 indicating a shorter potential collision time and a higher probability of collision.

RC represents the percentage of the planned route distance that has been successfully completed by AV. This metric employs the same calculation method as Equation 5 to assess the degree of violation of requirement $R2$. Its value ranges from 0 to 100, with values closer to 0 meaning lower completion of the route and a greater degree of $R2$ violation.

4.6 Statistical Tests

Given that the results of our experiment are dichotomous, i.e., a scenario violated both requirements (Yes or No), we employed the Fisher’s exact test [42] to determine the statistical significance of results based on the recommendations from [43], with a significance level of $p < 0.05$. For the effect size, we chose odds ratios (OR) [44] based on an existing guide [43]. When OR is 1, the two compared methods are equal. An OR greater than 1 suggests that the first method is more likely to be better than the second, while an OR less than 1 indicates the opposite. The further the OR deviates from 1, the stronger the effect.

5 Analysis of the Results and Discussion

5.1 Results for RQ1 – Comparison with RS

We compared $MOEQT$ with RS regarding the three violation metrics, i.e., V_{R1} , V_{R2} , and V_{R1_R2} . Besides, we also employed the mean TTC and mean RC to evaluate each method regarding the abilities to optimize objectives.¹ Table 1 presents the descriptive statistics of $MOEQT$ compared to RS on the six roads. We also report the Fisher’s exact test results in Table 2.

Regarding V_{R1} , Table 1 shows that $MOEQT$ outperformed RS on *Road1*, *Road2*, and *Road4*. For *Road5* and *Road6*, both $MOEQT$ and RS achieved equivalent performance, while on *Road3*, RS resulted in six violations of requirement $R1$, outperforming $MOEQT$, which achieved two $R1$ violations. As for the statistical results, the results in Table 2 demonstrated that $MOEQT$ outperformed RS on *Road1*, *Road2*, and *Road4*. For *Road3*, *Road5*, and *Road6*, no significant differences were observed. This indicates that $MOEQT$ consistently performed similarly to or better than RS across the various roads. We further calculated the mean TTC of scenarios that violated $R1$ (i.e., $TTC_{V_{R1}}$), and we observe that $MOEQT$ performed better than RS on *Road1*, *Road2*, and *Road4*. Similarly, RS outperformed $MOEQT$ on *Road3*. On *Road6*, although both methods exhibited identical performance for V_{R1} , $MOEQT$ surpassed RS in $TTC_{V_{R1}}$, indicating that the two methods identified different scenarios violating the same requirement $R1$. For *Road5*, no scenario was found that violated $R1$, making $TTC_{V_{R1}}$ inapplicable for both $MOEQT$ and RS .

For V_{R2} , $MOEQT$ significantly outperformed RS on *Road1*, *Road3*, *Road4*, and *Road6* in terms of violating the requirement $R2$. On *Road2* and *Road5*, however, RS performed slightly better than $MOEQT$, with differences of 2 and 4 violation scenarios, respectively. As similarly shown in Table 2, $MOEQT$ demonstrated significant superiority over RS on *Road1*, *Road3*, *Road4*, and *Road6*, while performing comparably with RS on *Road2* and *Road5*. This highlights that across all roads, $MOEQT$ was either superior (4 out of 6) or equal (2 out of 6) to RS . Considering $RC_{V_{R2}}$, $MOEQT$ performed better than RS on all roads except *Road5*, where $MOEQT$ didn’t generate scenarios that violated $R2$. It means that the critical scenarios produced by $MOEQT$ demonstrated a greater degree of violation compared to those of RS , highlighting $MOEQT$ ’s clear tendency to target and violate requirement $R2$ based on its violation objective.

¹Note that we obtain each TTC for each scenario by averaging the TTC at each time step, and the $TTC_{V_{R1}}$ values reported in Table 1 are the mean values of all scenarios where $R1$ violation occurred. Similarly, $RC_{V_{R2}}$ are the mean values of all scenarios where $R2$ violation occurred. For $TTC_{V_{R1_R2}}$ and $RC_{V_{R1_R2}}$, we consider scenarios where both $R1$ and $R2$ were violated.

Table 1: Descriptive Statistics achieved by *RS*, *SORLW*, and *MOEQT* for Different Roads. “/” means not applicable. **Bold** indicates the best result across all the methods.

Road	Method	Evaluation Metric						
		$V_{R1} \uparrow$	$TTC_{V_{R1}} \downarrow$	$V_{R2} \uparrow$	$RC_{V_{R2}} \downarrow$	$V_{R1_R2} \uparrow$	$TTC_{V_{R1_R2}} \downarrow$	$RC_{V_{R1_R2}} \downarrow$
Road1	<i>RS</i>	3	9.289	33	90.424	1	11.305	96.871
	<i>SORLW</i>	0	/	24	93.090	0	/	/
	<i>MOEQT</i>	25	5.424	66	80.184	17	6.278	85.276
Road2	<i>RS</i>	4	9.071	20	47.290	4	9.071	44.806
	<i>SORLW</i>	0	/	2	94.481	0	/	/
	<i>MOEQT</i>	15	0.000	18	27.942	15	0.000	28.248
Road3	<i>RS</i>	6	11.772	24	66.833	6	11.772	77.890
	<i>SORLW</i>	0	/	54	95.702	0	/	/
	<i>MOEQT</i>	2	14.167	75	59.157	2	14.167	83.423
Road4	<i>RS</i>	5	6.756	30	58.952	5	6.756	70.147
	<i>SORLW</i>	0	/	99	55.019	0	/	/
	<i>MOEQT</i>	34	0.963	82	56.868	33	0.959	64.694
Road5	<i>RS</i>	0	/	4	77.595	0	/	/
	<i>SORLW</i>	0	/	0	/	0	/	/
	<i>MOEQT</i>	0	/	0	/	0	/	/
Road6	<i>RS</i>	1	13.333	30	79.966	1	13.333	87.567
	<i>SORLW</i>	0	/	22	92.465	0	/	/
	<i>MOEQT</i>	1	7.612	55	64.728	1	7.612	87.567

Table 2: Fisher’s Exact Test Statistical Results of *MOEQT* Compared with *RS* on Different Roads. “/” means not applicable. Underlining denotes that the statistical results are not significantly different.

Metric	Statistic	Road					
		<i>Road1</i>	<i>Road2</i>	<i>Road3</i>	<i>Road4</i>	<i>Road5</i>	<i>Road6</i>
V_{R1}	<i>p</i>	<0.01	<0.05	<u>≥ 0.05</u>	<0.01	<u>≥ 0.05</u>	<u>≥ 0.05</u>
	<i>OR</i>	10.778	4.235	<u>0.320</u>	9.788	/	<u>1.000</u>
V_{R2}	<i>p</i>	<0.01	<u>≥ 0.05</u>	<0.01	<0.01	<u>≥ 0.05</u>	<0.01
	<i>OR</i>	3.941	<u>0.878</u>	9.500	10.630	<u>0.000</u>	2.852
V_{R1_R2}	<i>p</i>	<0.01	<0.05	<u>≥ 0.05</u>	<0.01	<u>≥ 0.05</u>	<u>≥ 0.05</u>
	<i>OR</i>	20.277	4.235	<u>0.320</u>	9.358	/	<u>1.000</u>

Regarding V_{R1_R2} , Table 1 shows that *MOEQT* led to more critical scenarios violating *R1* and *R2* simultaneously on *Road1*, *Road2*, and *Road4*, while neither *MOEQT* nor *RS* on *Road5* violated both requirements simultaneously. On *Road6*, both *MOEQT* and *RS* generated only one scenario that violated both requirements, while on *Road3*, *RS* generated more scenarios to violate both requirements than *MOEQT*, although the difference was small, i.e., 6 vs. 2. We further analyzed the generated critical scenarios on each road and found that the number of violations of the two requirements on *Road3*, *Road5*, and *Road6* was small because it was difficult to violate *R1* on these three roads. Specifically, for *MOEQT*, the numbers of violations of *R1* on *Road3*, *Road5*, and *Road6* were 2, 0, 1, respectively. After replaying the scenarios and analyzing these roads, we found that these roads have more complex structures compared to other roads, causing the AV to drive more cautiously, especially for *Road5* which mainly contains intersections. For *RS*, the number of violations was 6, 0, and 1, respectively. Regarding the statistical test results, as Table 2 shows, *MOEQT* significantly outperformed *RS* on *Road1*, *Road2*, and *Road4*, and achieved a comparable performance as *RS* on the other roads. The results of V_{R1_R2} indicate that *MOEQT* achieved an overall better performance than *RS* in terms of violating both requirements simultaneously, but the performance varies across different roads. When it comes to mean $TTC_{V_{R1_R2}}$ when both *R1* and *R2* were violated, the results in Table 1 show that *MOEQT* outperformed *RS* with lower mean $TTC_{V_{R1_R2}}$ on *Road1*, *Road2*, *Road4*, and *Road6*. For *Road3*, *RS* was better than *MOEQT* (11.772 vs. 14.167). Moreover, no method violated both requirements on *Road5*. Similarly, regarding mean $RC_{V_{R1_R2}}$, as Table 1 shows, *MOEQT* outperformed *RS* on *Road1*, *Road2*, and *Road4*, while being equal on *Road6*. For *Road3*, *RS* was better than *MOEQT*, whereas no violations were detected on *Road5*. The results for $TTC_{V_{R1_R2}}$ and $RC_{V_{R1_R2}}$ show that for critical scenarios that violate these two requirements, the scenarios generated by *MOEQT* make it more difficult for the AV to complete its route and lead to a higher risk of collision.

Table 3: Fisher’s Exact Test Statistical Results of *MOEQT* Compared with *SORLW* on Different Roads. “*inf*” represents infinity. “/” means not applicable. Underlining denotes that the statistical results are not significantly different.

Metric	Statistic	Road					
		Road1	Road2	Road3	Road4	Road5	Road6
V_{R2}	p	<0.01	<0.01	<0.01	<0.01	<u>≥ 0.05</u>	<0.01
	OR	6.147	10.756	2.556	0.046	/	4.333

Conclusion for RQ1: *MOEQT* achieved an overall better performance than *RS* in terms of violating the single requirement or both requirements simultaneously, and the scenarios generated by *MOEQT* make it harder for the AV to complete its route and increase the risk of collision.

5.2 Results for RQ2 – Comparison with *SORLW*

Table 1 presents the descriptive statistics of *MOEQT* compared to *SORLW* on each of the six roads. As the table shows, in terms of the number of scenarios that violated *R1* or violated *R1* and *R2* at the same time, i.e., V_{R1} and V_{R1_R2} , *MOEQT* outperformed *SORLW* on all of the six roads except for *Road5*, where neither *MOEQT* nor *SORLW* violated both requirements. When checking the specific numbers, we found that *SORLW* did not generate any scenario that violated the requirement *R1* or violated both requirements simultaneously on all six roads. One possible explanation is that *SORLW* used fixed equal weights during the optimization process, which prevents *SORLW* from dynamically adjusting the importance of each objective based on the current environment state. Therefore, the *SORLW* agent may struggle to adaptively balance objectives with different levels of importance, leading to a local optimum, where the reward for one objective is maximized at the expense of the other. Since *SORLW* generated zero critical scenarios for both the V_{R1} and V_{R1_R2} metrics across all roads, conducting Fisher’s exact test to compare it with *MOEQT* was not meaningful and was therefore omitted.

We further compared *SORLW* with *MOEQT* regarding V_{R2} . As shown in Table 1, *MOEQT* outperformed *SORLW* on *Road1*, *Road2*, *Road3*, and *Road6*. On *Road4*, however, *SORLW* performed better than *MOEQT*, with specific V_{R2} values of 99 and 82, respectively. For *Road5*, neither method generated critical scenarios violating requirement *R2*. Similarly, Table 3 indicates that on *Road1*, *Road2*, *Road3*, and *Road6*, *MOEQT* was significantly better than *SORLW*. While for *Road4*, *SORLW* showed superior performance, with the p -value less than 0.01 and the OR value of 0.046 (less than 1). On *Road5*, there were no significant differences between the two methods.

Conclusion for RQ2: The results show that *MOEQT* outperformed *SORLW* regarding generating critical scenarios to violate multiple requirements simultaneously, indicating that MORL is more effective in handling AV testing tasks where multiple test objectives need to be satisfied.

5.3 Discussion

Benefiting from adaptive weights. Multiple objectives must be adaptively balanced during training due to their inherent interdependencies. Figure 3 shows the convergence trends of the two objectives ($TTC_{V_{R1_R2}}$ and $RC_{V_{R1_R2}}$) achieved by *MOEQT* and *SORLW* during training on the six roads. As the figure shows, on *Road1*, *MOEQT* converged to a lower $TTC_{V_{R1_R2}}$ and lower $RC_{V_{R1_R2}}$ compared to *SORLW*. Moreover, compared to *SORLW*, *MOEQT* was more stable throughout the training process, with *SORLW* showing no clear convergence trend for TTC , indicating that *MOEQT* achieved a better balance between the two objectives. On *Road2*, though both *MOEQT* and *SORLW* converged to a similar $TTC_{V_{R1_R2}}$ and $RC_{V_{R1_R2}}$, we observed that *MOEQT* was more efficient in finding the optimal solutions. In addition, compared to *SORLW*, *MOEQT* was more stable and better balancing the two objectives during the training process. On *Road3*, *MOEQT* converged to a lower $TTC_{V_{R1_R2}}$ and a similar $RC_{V_{R1_R2}}$ compared to *SORLW*. As for the training stability, *MOEQT* was more stable than *SORLW*, indicating a better balance between the two objectives. For *Road4*, *MOEQT* and *SORLW* converged to a similar $TTC_{V_{R1_R2}}$ and $RC_{V_{R1_R2}}$, while *SORLW* was worse regarding training stability. On *Road5*, regarding $TTC_{V_{R1_R2}}$ convergence, *MOEQT* was slightly worse than *SORLW*, but it achieved a faster convergence speed. Furthermore, in terms of $RC_{V_{R1_R2}}$, we did not observe a convergence trend for *SORLW*, while *MOEQT* converged. This observation indicates that the objectives were better balanced by *MOEQT*, whereas *SORLW* failed to adaptively balance the importance of the two objectives, resulting in only one objective being optimized. On *Road6*, we observed that both methods converged to a similar $TTC_{V_{R1_R2}}$ and $RC_{V_{R1_R2}}$. Besides, although both methods tend to focus more on $TTC_{V_{R1_R2}}$, *MOEQT* performed more stable during training. Long story

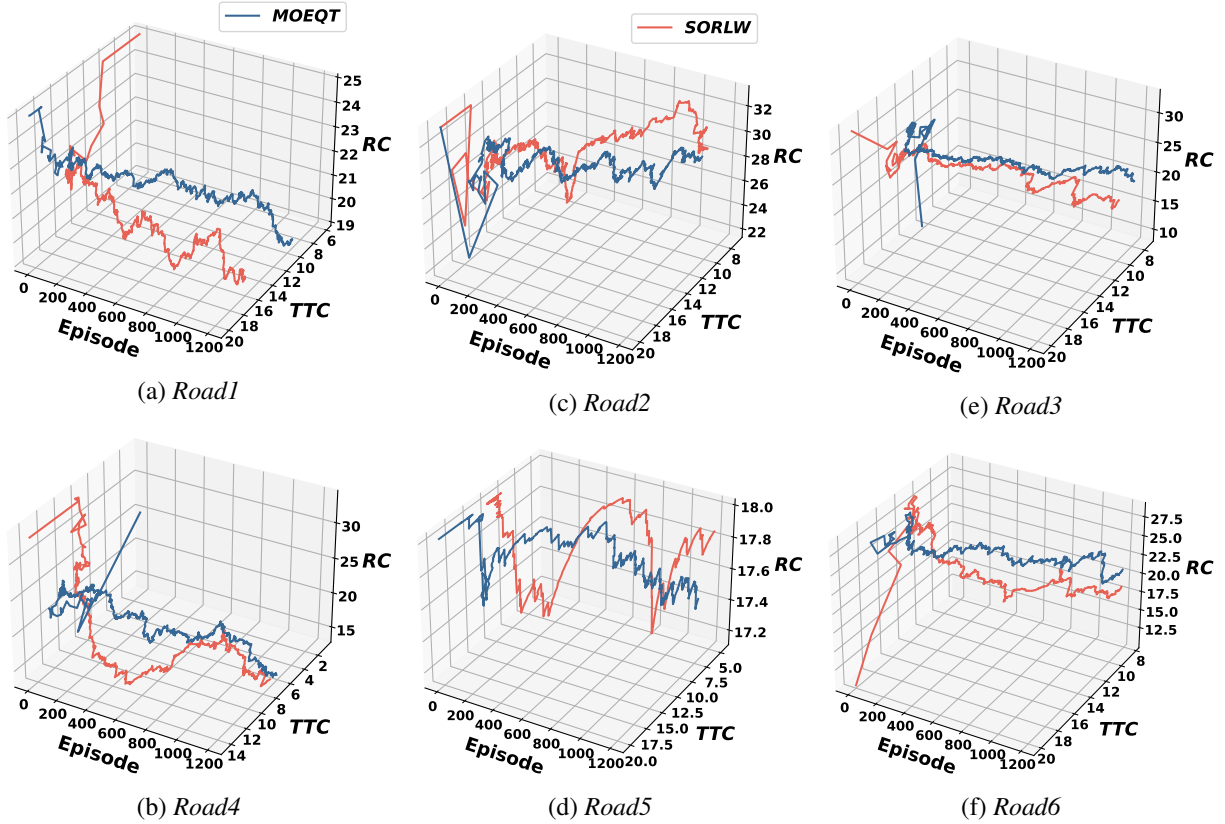


Figure 3: Convergence Trends of TTC and RC achieved by $MOEQT$ and $SORLW$ on Different Roads.

short, $MOEQT$ achieved an overall stable performance during training and well-balanced the two objectives, indicating that MORL with an adaptive weighting mechanism can better handle these two objectives compared to single-objective RL with fixed equal weights.

Analyzing violations of requirements. Recall that our goal is to generate scenarios that violate multiple requirements simultaneously, and the evaluation results show that $MOEQT$ tends to have a higher chance of violating two requirements simultaneously. To understand how $MOEQT$ performed in violating every individual requirement, we further analyze the distribution of violations of each requirement. As shown in Table 1, the results indicate that for the scenarios generated by all three methods, $R2$ is more easily violated than $R1$. For example, on *Road1*, the numbers of scenarios that violated $R1$ are 3, 0, and 25 for RS , $SORLW$, and $MOEQT$, respectively, while as for scenarios that violated $R2$, the numbers are 33, 24, and 66 for RS , $SORLW$, and $MOEQT$, respectively. Similar observations can be found on the other roads, where $R2$ is more likely to be violated than $R1$. A plausible explanation is that the AV under test is designed to prioritize $R1$ (collision avoidance), as collisions tend to result in more severe consequences compared to not completing a route ($R2$). The emphasis on safety makes the AV more robust to $R1$ violations but may overlook the functional requirement, i.e., $R2$, making it more vulnerable to route completion failures. This observation highlights the importance of striking a balance between safety and functional requirements in AV design and the need for a more holistic approach that weighs these requirements effectively.

6 Threats to Validity

Conclusion validity is concerned with the reliability of the conclusion drawn from the empirical study, which might be influenced by the inherent randomness of the simulator. We mitigate this threat by repeating each execution 100 times and using appropriate statistical tests following well-known guidelines [43]. *Construct validity* relates to the evaluation metrics. For a fair comparison, we chose five metrics commonly used for AV testing. We also employed comparable metrics to evaluate the performance of RL and MORL algorithms. *Internal validity* concerns with the parameter settings. To mitigate the potential threats to internal validity, we determined the hyperparameters by employing an automated hyperparameter optimization framework named Optuna [38]. Besides, we acknowledge the performance of $MOEQT$

might be improved by tuning EQL settings, e.g., formulating the state space using sensor data such as camera images, and designing action space covering more environmental objects. Thus, we will investigate other *MOEQT* designs in the future. *External validity* is about the generalizability of the empirical evaluation. We used one subject system and one simulator to conduct the experiment, which could potentially threaten the external validity. To mitigate this issue, we chose the advanced end-to-end AV controller (i.e., Interfuser) and the high-fidelity simulator (i.e., CARLA). However, we acknowledge that conducting experiments with more case study systems could strengthen our conclusions. *MOEQT* can be easily adapted to test other AV systems with minimal effort.

7 Related Work

Testing AVs in various driving scenarios is critical in ensuring their safety and functionality. However, due to the complexity of the AV operating environments, there is theoretically an infinite number of possible driving scenarios. Therefore, we need to identify critical scenarios that could violate safety or functional requirements. Search-based methods are widely adopted to generate critical scenarios under the guidance of fitness functions [45, 46, 9, 10, 11, 12]. For example, Abdesslem et al. [46] proposed NSGAI-DT to test vision-based control systems by combining NSGAI-II [47] and decision tree models. Li et al. [48] proposed AV-Fuzzer, an approach integrating fuzz testing with evolutionary search, to identify critical scenarios that cause safety violations. Haq et al. [49] proposed SAMOTA, an efficient AV testing approach that combines multi-objective search with surrogate models. SAMOTA employs multi-objective search to generate critical scenarios and improves testing efficiency by simulating the simulator with surrogate models. To test AV against traffic laws, Sun et al. [50] proposed LawBreaker, which adopts a fuzzing algorithm to search for scenarios that can effectively violate traffic laws. Though search-based approaches have shown promising performance, they have limited effectiveness in handling tasks requiring runtime sequential interactions with the environment, which are essential when manipulating dynamic objects and ensuring precise control over them. Another challenge is that the AV operating environment is dynamically changing and uncertain, while search-based approaches cannot effectively adapt to environmental changes.

RL-based approaches generate critical scenarios through intelligent agents that interact with and configure the AV operating environment [51, 14, 15, 16]. For example, Koren et al. [52] extended adaptive stress testing using RL to find critical scenarios that cause AV to collide. Lu et al. [14] proposed DeepCollision, an RL-based environment configuration framework that generates scenarios to uncover collisions of AV. To test lane-changing models, Chen et al. [51] proposed an RL-based adaptive testing framework to generate time-sequential adversarial scenarios. Similarly, Doreste et al [53] proposed an adversarial method that models NPCs with independent RL-based agents to challenge the ADS under test. Feng et al. [16] proposed a dense RL-based approach to learn critical scenarios from naturalistic driving data by editing the Markov decision process to eliminate non-safety-critical states. To test multiple requirements, Haq et al. [15] proposed MORLOT that adapts single-objective RL and multi-objective search to generate test suites to violate as many requirements as possible. Notice that MORLOT is designed to violate multiple *independent* requirements by developing a set of scenarios, each violating one independent requirement. However, in reality, AV requirements are often interdependent and must be evaluated simultaneously. For example, failing to meet a functional requirement (e.g., not completing a route) may violate a safety requirement (e.g., causing a crash), highlighting the need for approaches simultaneously evaluating multiple requirements.

Different from the above works, we propose *MOEQT* by applying MORL to generate critical scenarios that violate multiple requirements simultaneously. *MOEQT* relies on EQL to automatically learn and adaptively generate critical scenarios by interacting with AV operating environments through a multi-objective approach.

8 Conclusion and Future Work

In practice, many Autonomous Vehicle (AV) requirements are inherently interdependent and must be evaluated simultaneously to ensure comprehensive testing. To this end, we propose *MOEQT*, a multi-objective reinforcement learning (MORL)-based AV testing approach to generate critical scenarios violating multiple requirements simultaneously. *MOEQT* employs the Envelope Q-learning algorithm to adaptively learn environment configurations that lead to violations of multiple requirements. We select two common AV requirements for evaluation and compare *MOEQT* with two baseline methods on six driving roads covering different driving situations. The evaluation results demonstrate the promising performance of *MOEQT* in generating scenarios to test interdependent AV requirements. In the future, we plan to investigate the generalization of *MOEQT* by systematically conducting experiments with different AVs and simulators. Besides, we plan to study *MOEQT*'s effectiveness in testing other AV requirements. Finally, investigating other *MOEQT* designs such as adapting multiple policy MORL algorithms is another further plan. The replication package is provided in an online repository [39].

Acknowledgments

This work is supported by the Co-tester project (No. 314544) and the Co-evolver project (No. 286898/F20), funded by the Research Council of Norway. The work is also partially supported by the RoboSAPIENS project funded by the European Commission’s Horizon Europe programme under grant agreement number 101133807. Aitor Arrieta is part of the Software and Systems Engineering research group of Mondragon Unibertsitatea (IT1519-22), supported by the Department of Education, Universities and Research of the Basque Country.

References

- [1] Xinhai Zhang, Jianbo Tao, Kaige Tan, Martin Törngren, José Manuel Gaspar Sánchez, Muhammad Rusyadi Ramli, Xin Tao, Magnus Gyllenhammar, Franz Wotawa, Naveen Mohan, et al. Finding critical scenarios for automated driving systems: A systematic mapping study. *IEEE Transactions on Software Engineering*, 49(3):991–1026, 2022.
- [2] Wenhao Ding, Chejian Xu, Mansur Arief, Haohong Lin, Bo Li, and Ding Zhao. A survey on safety-critical driving scenario generation—a methodological perspective. *IEEE Transactions on Intelligent Transportation Systems*, 24(7):6971–6988, 2023.
- [3] Andrea Stocco, Brian Pulfer, and Paolo Tonella. Mind the gap! a study on the transferability of virtual versus physical-world testing of autonomous driving systems. *IEEE Transactions on Software Engineering*, 49(4):1928–1940, 2022.
- [4] Andrea Stocco, Brian Pulfer, and Paolo Tonella. Model vs system level testing of autonomous driving systems: a replication and extension study. *Empirical Software Engineering*, 28(3):73, 2023.
- [5] Mahshid Helali Moghadam, Markus Borg, Mehrdad Saadatmand, Seyed Jalaleddin Mousavirad, Markus Bohlin, and Björn Lisper. Machine learning testing in an adas case study using simulation-integrated bio-inspired search-based testing. *Journal of Software: Evolution and Process*, 36(5):e2591, 2024.
- [6] Neelofar Neelofar and Aldeida Aleti. Identifying and explaining safety-critical scenarios for autonomous vehicles via key features. *ACM Transactions on Software Engineering and Methodology*, 33(4):1–32, 2024.
- [7] Victor Crespo-Rodriguez, Neelofar, and Aldeida Aleti. Pafot: A position-based approach for finding optimal tests of autonomous vehicles. In *Proceedings of the 5th ACM/IEEE International Conference on Automation of Software Test (AST 2024)*, pages 159–170, 2024.
- [8] Alexey Dosovitskiy, German Ros, Felipe Codevilla, Antonio Lopez, and Vladlen Koltun. Carla: An open urban driving simulator. In *Conference on robot learning*, pages 1–16. PMLR, 2017.
- [9] Ziyuan Zhong, Gail Kaiser, and Baishakhi Ray. Neural network guided evolutionary fuzzing for finding traffic violations of autonomous vehicles. *IEEE Transactions on Software Engineering*, 49(4):1860–1875, 2022.
- [10] Chengjie Lu, Shaikat Ali, and Tao Yue. Epitester: Testing autonomous vehicles with epigenetic algorithm and attention mechanism. *IEEE Transactions on Software Engineering*, pages 1–19, 2024.
- [11] Yuqi Huai, Sumaya Almanee, Yuntianyi Chen, Xiafa Wu, Qi Alfred Chen, and Joshua Garcia. scenorita: Generating diverse, fully mutable, test scenarios for autonomous vehicle planning. *IEEE Transactions on Software Engineering*, 49(10):4656–4676, 2023.
- [12] Yuan Zhou, Yang Sun, Yun Tang, Yuqi Chen, Jun Sun, Christopher M Poskitt, Yang Liu, and Ziji Yang. Specification-based autonomous driving system testing. *IEEE Transactions on Software Engineering*, 49(6):3391–3410, 2023.
- [13] Richard S Sutton and Andrew G Barto. *Reinforcement learning: An introduction*. MIT press, 2018.
- [14] Chengjie Lu, Yize Shi, Huihui Zhang, Man Zhang, Tiexin Wang, Tao Yue, and Shaikat Ali. Learning configurations of operating environment of autonomous vehicles to maximize their collisions. *IEEE Transactions on Software Engineering*, 49(1):384–402, 2022.
- [15] Fitash Ul Haq, Donghwan Shin, and Lionel C. Briand. Many-objective reinforcement learning for online testing of dnn-enabled systems. In *2023 IEEE/ACM 45th International Conference on Software Engineering (ICSE)*, pages 1814–1826, 2023.
- [16] Shuo Feng, Haowei Sun, Xintao Yan, Haojie Zhu, Zhengxia Zou, Shengyin Shen, and Henry X Liu. Dense reinforcement learning for safety validation of autonomous vehicles. *Nature*, 615(7953):620–627, 2023.
- [17] Chunming Liu, Xin Xu, and Dewen Hu. Multiobjective reinforcement learning: A comprehensive overview. *IEEE Transactions on Systems, Man, and Cybernetics: Systems*, 45(3):385–398, 2015.

- [18] Conor F Hayes, Roxana Rădulescu, Eugenio Bargiacchi, Johan Källström, Matthew Macfarlane, Mathieu Reymond, Timothy Verstraeten, Luisa M Zintgraf, Richard Dazeley, Fredrik Heintz, et al. A practical guide to multi-objective reinforcement learning and planning. *Autonomous Agents and Multi-Agent Systems*, 36(1):26, 2022.
- [19] Jie Xu, Yunsheng Tian, Pingchuan Ma, Daniela Rus, Shinjiro Sueda, and Wojciech Matusik. Prediction-guided multi-objective reinforcement learning for continuous robot control. In *International conference on machine learning*, pages 10607–10616. PMLR, 2020.
- [20] B Ravi Kiran, Ibrahim Sobh, Victor Talpaert, Patrick Mannion, Ahmad A Al Sallab, Senthil Yogamani, and Patrick Pérez. Deep reinforcement learning for autonomous driving: A survey. *IEEE Transactions on Intelligent Transportation Systems*, 23(6):4909–4926, 2021.
- [21] Runzhe Yang, Xingyuan Sun, and Karthik Narasimhan. A generalized algorithm for multi-objective reinforcement learning and policy adaptation. *Advances in neural information processing systems*, 32, 2019.
- [22] Hao Shao, Letian Wang, Ruobing Chen, Hongsheng Li, and Yu Liu. Safety-enhanced autonomous driving using interpretable sensor fusion transformer. In *Conference on Robot Learning*, pages 726–737. PMLR, 2023.
- [23] Christopher JCH Watkins and Peter Dayan. Q-learning. *Machine learning*, 8:279–292, 1992.
- [24] Diederik M Roijers, Peter Vamplew, Shimon Whiteson, and Richard Dazeley. A survey of multi-objective sequential decision-making. *Journal of Artificial Intelligence Research*, 48:67–113, 2013.
- [25] Florian Felten, Lucas N Alegre, Ann Nowe, Ana Bazzan, El Ghazali Talbi, Grégoire Danoy, and Bruno C da Silva. A toolkit for reliable benchmarking and research in multi-objective reinforcement learning. *Advances in Neural Information Processing Systems*, 36, 2024.
- [26] Volodymyr Mnih, Koray Kavukcuoglu, David Silver, Andrei A Rusu, Joel Veness, Marc G Bellemare, Alex Graves, Martin Riedmiller, Andreas K Fidjeland, Georg Ostrovski, et al. Human-level control through deep reinforcement learning. *nature*, 518(7540):529–533, 2015.
- [27] Layne T Watson and Raphael T Haftka. Modern homotopy methods in optimization. *Computer Methods in Applied Mechanics and Engineering*, 74(3):289–305, 1989.
- [28] Tom Schaul. Prioritized experience replay. *arXiv preprint arXiv:1511.05952*, 2015.
- [29] Edouard Leurent. A survey of state-action representations for autonomous driving. 2018.
- [30] A Vaswani. Attention is all you need. *Advances in Neural Information Processing Systems*, 2017.
- [31] S Phaniteja, Parijat Dewangan, Pooja Guhan, Abhishek Sarkar, and K Madhava Krishna. A deep reinforcement learning approach for dynamically stable inverse kinematics of humanoid robots. In *2017 IEEE international conference on robotics and biomimetics (ROBIO)*, pages 1818–1823. IEEE, 2017.
- [32] Long Chen, Xuemin Hu, Bo Tang, and Yu Cheng. Conditional dqn-based motion planning with fuzzy logic for autonomous driving. *IEEE Transactions on Intelligent Transportation Systems*, 23(4):2966–2977, 2020.
- [33] Cumhur Erkan Tuncali, Georgios Fainekos, Danil Prokhorov, Hisahiro Ito, and James Kapinski. Requirements-driven test generation for autonomous vehicles with machine learning components. *IEEE Transactions on Intelligent Vehicles*, 5(2):265–280, 2019.
- [34] Michiel M Minderhoud and Piet HL Bovy. Extended time-to-collision measures for road traffic safety assessment. *Accident Analysis & Prevention*, 33(1):89–97, 2001.
- [35] Wilko Schwarting, Javier Alonso-Mora, and Daniela Rus. Planning and decision-making for autonomous vehicles. *Annual Review of Control, Robotics, and Autonomous Systems*, 1(1):187–210, 2018.
- [36] CARLA Team, Intel Autonomous Agents Lab, Embodied AI Foundation, and AlphaDrive. Carla autonomous driving leaderboard. <https://leaderboard.carla.org>, 2024.
- [37] Chengjie Lu, Shaukat Ali, and Tao Yue. Epitester: Testing autonomous vehicles with epigenetic algorithm and attention mechanism. *IEEE Transactions on Software Engineering*, 2024.
- [38] Takuya Akiba, Shotaro Sano, Toshihiko Yanase, Takeru Ohta, and Masanori Koyama. Optuna: A next-generation hyperparameter optimization framework. In *Proceedings of the 25th ACM SIGKDD international conference on knowledge discovery & data mining*, pages 2623–2631, 2019.
- [39] Jiahui Wu, Chengjie Lu, Aitor Arrieta, and Shaukat Ali. MOEQT. <https://github.com/Simula-COMPLEX/MOEQT>, 2025.
- [40] Bradly C Stadie, Sergey Levine, and Pieter Abbeel. Incentivizing exploration in reinforcement learning with deep predictive models. *arXiv preprint arXiv:1507.00814*, 2015.

- [41] Wassim G Najm, John D Smith, Mikio Yanagisawa, et al. Pre-crash scenario typology for crash avoidance research. Technical report, United States. Department of Transportation. National Highway Traffic Safety . . . , 2007.
- [42] Ronald Aylmer Fisher. Statistical methods for research workers. In *Breakthroughs in statistics: Methodology and distribution*, pages 66–70. Springer, 1970.
- [43] Andrea Arcuri and Lionel Briand. A practical guide for using statistical tests to assess randomized algorithms in software engineering. In *Proceedings of the 33rd international conference on software engineering*, pages 1–10, 2011.
- [44] Magdalena Szumilas. Explaining odds ratios. *Journal of the Canadian academy of child and adolescent psychiatry*, 19(3):227, 2010.
- [45] Raja Ben Abdesslem, Shiva Nejati, Lionel C Briand, and Thomas Stifter. Testing advanced driver assistance systems using multi-objective search and neural networks. In *Proceedings of the 31st IEEE/ACM international conference on automated software engineering*, pages 63–74, 2016.
- [46] Raja Ben Abdesslem, Shiva Nejati, Lionel C Briand, and Thomas Stifter. Testing vision-based control systems using learnable evolutionary algorithms. In *Proceedings of the 40th International Conference on Software Engineering*, pages 1016–1026, 2018.
- [47] Kalyanmoy Deb, Amrit Pratap, Sameer Agarwal, and TAMT Meyarivan. A fast and elitist multiobjective genetic algorithm: Nsga-ii. *IEEE transactions on evolutionary computation*, 6(2):182–197, 2002.
- [48] Guanpeng Li, Yiran Li, Saurabh Jha, Timothy Tsai, Michael Sullivan, Siva Kumar Sastry Hari, Zbigniew Kalbarczyk, and Ravishankar Iyer. Av-fuzzer: Finding safety violations in autonomous driving systems. In *2020 IEEE 31st international symposium on software reliability engineering (ISSRE)*, pages 25–36. IEEE, 2020.
- [49] Fitash Ul Haq, Donghwan Shin, and Lionel Briand. Efficient online testing for dnn-enabled systems using surrogate-assisted and many-objective optimization. In *Proceedings of the 44th international conference on software engineering*, pages 811–822, 2022.
- [50] Yang Sun, Christopher M Poskitt, Jun Sun, Yuqi Chen, and Zijiang Yang. Lawbreaker: An approach for specifying traffic laws and fuzzing autonomous vehicles. In *Proceedings of the 37th IEEE/ACM International Conference on Automated Software Engineering*, pages 1–12, 2022.
- [51] Baiming Chen, Xiang Chen, Qiong Wu, and Liang Li. Adversarial evaluation of autonomous vehicles in lane-change scenarios. *IEEE transactions on intelligent transportation systems*, 23(8):10333–10342, 2021.
- [52] Mark Koren, Saud Alsaif, Ritchie Lee, and Mykel J. Kochenderfer. Adaptive stress testing for autonomous vehicles. In *2018 IEEE Intelligent Vehicles Symposium (IV)*, pages 1–7, 2018.
- [53] Andréa Doreste, Matteo Biagiola, and Paolo Tonella. Adversarial testing with reinforcement learning: A case study on autonomous driving. In *2024 IEEE Conference on Software Testing, Verification and Validation (ICST)*, pages 293–304. IEEE, 2024.